AD/A-007 147

SYSTEMATIC STUDY OF PYROELECTRICITY. FERROELECTRICITY AND PYROELECTRICITY IN THE PEROVSKITES

M. I. Bell, et al

Belfer Graduate School of Science

Prepared for:

Army Electronics Command
Advanced Research Projects Agency

January 1975

UNCLASSIFIED

SECURITY CLASSIFICATION OF THIS PAGE (When Data Entered)

REPORT DOCUMENTATION PAGE

READ INSTRUCTIONS BEFORE COMPLETING FORM

1. REPORT NUMBER: ECOM-74-0470-1	2. GOVT ACCESSION NO.
3. RECIPIENT'S CATALOG NUMBER	
4. TITLE (and Subtitle): SYSTEMATIC STUDY OF PYROELECTRICITY Ferroelectricity and Pyroelectricity in the Perovskites	5. TYPE OF REPORT & PERIOD COVERED: Technical Report 1 Oct 73 - 30 Sept 74
	6. PERFORMING ORG. REPORT NUMBER
7. AUTHOR(s): M. I. Bell and P. M. Raccah	8. CONTRACT OR GRANT NUMBER(s): DAAB 07-74-C-0470
9. PERFORMING ORGANIZATION NAME AND ADDRESS: Yeshiva University, Belfer Graduate School of Science, Amsterdam Ave. 186th St., New York, N.Y. 10033	10. PROGRAM ELEMENT, PROJECT, TASK AREA & WORK UNIT NUMBERS: Program Code No. 4010
11. CONTROLLING OFFICE NAME AND ADDRESS: Advanced Research Project Agency, 1400 Wilson Blvd. Rosslyn, VA 22209	12. REPORT DATE: January 1975
	13. NUMBER OF PAGES: 45
14. MONITORING AGENCY NAME & ADDRESS (if different from Controlling Office): US Army Electronics Command, Fort Monmouth, NJ 07703 AMSEL-TL-ES	15. SECURITY CLASS. (of this report): Unclassified
	15a. DECLASSIFICATION/DOWNGRADING SCHEDULE

16. DISTRIBUTION STATEMENT (of this Report)

Approved for public release; distribution unlimited

17. DISTRIBUTION STATEMENT (of the abstract entered in Block 20, if different from Report)

18. SUPPLEMENTARY NOTES

This research was supported by Advanced Research Projects Agency of the Department of Defense and was monitored by US Army Electronics Command under Contract No. DAAB-07-74-C-0470 (see reverse side)

19. KEY WORDS (Continue on reverse side if necessary and identify by block number)

Pyroelectric Detectors, Figure of Merit, Displacement and order-disorder ferroelectrics, Molecular field theory, First and second order phase transitions, Perovskites, and Raman Scattering

20. ABSTRACT (Continue on reverse side if necessary and identify by block number)

The relation between ferroelectricity and pyroelectricity in the perovskites is explored using Devonshire's phenomenological theory of ferroelectricity and a new microscopic theory obtained by generalizing the conventional molecular field theory. The Devonshire formalism yields results for the pyroelectric coefficient and the figures of merit for pyroelectric detectors in terms of the parameters which characterize the dielectric behavior and the ferroelectric phase transition. A simple thermodynamic relation for the

DD FORM 1 JAN 73 1473 EDITION OF 1 NOV 65 IS OBSOLETE

PRICES SUBJECT TO CHANGE

UNCLASSIFIED

SECURITY CLASSIFICATION OF THIS PAGE (When Data Entered)

18. Supplementary Notes (cont'd)

Effective Date of Contract - 1 October 1973

Contract Expiration Date - 30 September 1975

Amount of Contract - Total amount: $148,840
First year: $ 72,582
Second year: $ 76,258

ARPA Contractor: Yeshiva University
P.M. Raccah, Principal Investigator
(212) 568-8400

Project Scientist: FREDERICK ROTHWARF
(201) 535-1407

20. Abstract (cont'd)

figure of merit is also derived. The molecular field theory is generalized in a novel way which permits it to describe first as well as second-order phase transitions. Good agreement with experiment is obtained for $BaTiO_3$. The new theory assumes the existence of a disordered array of dipoles in the perovskites, and evidence for this disorder is obtained from measurements of Raman scattering in $KNbO_3$.

CONTENTS

I. INTRODUCTION

The work described in this report was conducted from 1 October 1973 to 30 September 1974 under Advanced Research Projects Agency Contract DAAB 07-74-C-0470, P.M. Raccah, principal investigator, F. Rothwarf, contract monitor. Its purpose was to improve our understanding of the phenomenon of pyroelectricity through an exploration of the fundamental physical processes involved. It is hoped that such improved understanding will lead to practical guidelines for the selection of materials for use in infrared detectors and to useful insights into the factors limiting the performance of devices employing the pyroelectric effect.

The ferroelectric perovskites were chosen as a focus for this investigation since their properties have been extensively studied, and they provide a family of isomorphous materials in which the effects of varying certain physical parameters can be examined systematically.

The pyroelectric behavior of the pervoskites is intrinsically related to their ferroelectric behavior. Below the Curie temperature these crystals are spontaneously polarized, and although this polarization is always screened by stray charges attracted to the crystal, any change in temperature produces a change in the polarization of the crystal which appears as a net dipole moment and which persists until it can be compensated by a gain or loss of stray charge at the surfaces. This pyroelectric effect can be described by any theory of ferroelectricity which accounts for the temperature dependence of the spontaneous polarization. We have examined the simple thermodynamic theory due to Devonshire, and obtained from it several new results (Section II) which yield the pyroelectric coefficient and the figures of merit for pyroelectric detectors in terms of the parameters of that theory or in terms of simple (but at present less useful) thermodynamic relations. Section III describes our search for a microscopic calculation of the parameters appearing in Devonshire's theory. We obtain

the perhaps surprising result that a suitable generalization of the mean field theory so familiar in ferromagnetism can be used here with considerable success. The generalization required allows the theory to describe first-order as well as second-order transitions, and thus represents an interesting contribution to the general theory of phase transitions as well as a partial solution to the present problem. In justifying the use of a mean field theory, we must overcome the objection that the symmetry of the high-temperature phase does not permit the existence of the permanent dipole moments assumed in the theory. A variety of experimental evidence for the existence of a partially disordered array of dipoles in the pervoskites is presented, including our own measurements of Raman scattering in $KNbO_3$. Finally, Section IV describes additional experiments now in progress which may yield further evidence for the order-disorder nature of the phase transitions and outlines some new theoretical ideas which, although still speculative, show promise of greatly enhancing the power of the mean field theory.

II. THERMODYNAMIC THEORY

Devonshire's thermodynamic theory of ferroelectricity[1,2] can be used as the basis for a description of the pyroelectric effect in the perovskites. Part A of this section describes the free energy function introduced by Devonshire and summarizes the well-known results obtained from that function. Part B employs Devonshire's formalism to obtain expressions for the pyroelectric coefficient and the figures of merit relevant to the operation of pyroelectric detectors. These latter results, while simple, do not appear to have been discussed previously.

A. The Free Energy. If we restrict our attention to the transition from a non-polar (paraelectric) phase having inversion symmetry to a polar (ferroelectric) phase and consider only polarizations P along the polar axis, then the free energy at zero stress can be expanded[1] in a power series in P^2:

$$G = \tfrac{1}{2} A P^2 + \tfrac{1}{4} B P^4 + \tfrac{1}{6} C P^6 + \ldots , \qquad (1)$$

where the coefficients A, B, C,... are functions of the temperature. (Strictly speaking, the free energy G at non-zero stress is the elastic Gibbs function.[1]) The applied electric field is given by

$$E = \partial G/\partial P = AP + BP^3 + CP^5 + \ldots , \qquad (2)$$

and the dielectric stiffness (reciprocal of the susceptibility χ) is

$$1/\chi = \partial^2 G/\partial P^2 = A + 3BP^2 + 5\,CP^4 + \ldots . \qquad (3)$$

For the susceptibility of the paraelectric (P=0) phase to exhibit a Curie-Weiss behavior, it is sufficient to assume

$$A = A_o(T-T_o), \tag{4}$$

where T is the absolute temperature and T_o is the Curie-Weiss temperature (For $\chi \gg 1$, the usual Curie coefficient is then approximately $2\pi/A_c$). Most discussions of the thermodynamic theory[2] further assume that the higher-order Devonshire coefficients, B,C,... are temperature-independent and that the expansion of G in Eq. (1) can be cut off at the term proportional to P^6. Since the first assumption is contrary to the results of the microscopic model to be presented in Section III, we will avoid its use. The second assumption so greatly simplifies the theory that we will adopt it here, with the warning that our analysis of the experimental data for $BaTiO_3$ raises some doubt as to its validity. We should also note that this approximation for G requires $C > 0$ in order to prevent the minimum of G from occurring at infinite polarization. Equations such as (1)-(3) which are correct to all orders in P will have that fact indicated by the continuation sign (...).

Conditions for the existence of a spontaneous polarization in the absence of an applied field can be obtained from Eqs. (1)-(4). If terms of order P^8 and higher in G are neglected, then Eq.(2) with $E = 0$ has the solutions $P = 0$ and $P = P_s$, where

$$P_s^2 = - B/2C \left(1 \pm \sqrt{1-4AC/B^2}\right). \tag{5}$$

In order to have P_s real we must have $4AC/B^2 \leq 1$. Hence no polar state is possible at temperatures higher than T_u, where T_u is the solution of $4AC/B^2 = 1$. (For A given by Eq.(4) and B,C independent of T, we obtain the usual result[2], $T_u = T_o + B^2/4A_oC$.) For the polar state to be stable (or metastable) we must have $G(P_s)$ be a local minimum of G, and hence

$\partial^2 G/\partial P^2 = 1/\chi > 0$. This requires the choice of the plus (minus) sign in Eq.(5) if B is negative (positive).

We must now consider separately the cases $B > 0$ and $B < 0$. If $B > 0$ we have $P_s = 0$ at $T = T_o$, and P_s^2 is negative for $T_o < T < T_u$. Hence no spontaneous polarization is possible above T_o, and for $T < T_o$ the polarization increases continuously from zero, giving rise to a second-order transition. For $B < 0$, spontaneous polarization is possible for $T_o < T < T_u$, but the polar state is metastable as long as $G(P_s) > G(0) = 0$. The phase transition occurs at the Curie temperature T_c, at which $G(P_s) = 0$. Using Eqs.(1) and (2) with $G = E = 0$, we obtain

$$P_s^2 = -3B/4C, \quad \text{at } T = T_c \ . \tag{6}$$

Since the polar state has a finite polarization at T_c, the transition is first-order. Combining Eqs. (5) and (6) yields

$$A = 3B^2/16C \ , \text{ at } T = T_c \ . \tag{7}$$

(For A given by Eq.(4) and B,C independent of T, Eq. (7) gives the usual result[2], $T_c = T_o + 3B^2/16\, A_o C$.)

Equations (6) and (7) can be used to compare the susceptibilities χ_p and χ_f of the paraelectric and ferroelectric phases, respectively[3]. From Eq. (3) we have

$$1/\chi_p = A$$

$$1/\chi_f = A + 3BP_s^2 + 5\, C\, P_s^4 .$$

Direct substitution of Eqs. (6) and (7) gives

$$\chi_p = 4\, \chi_f \ , \qquad \text{at } T = T_c \tag{9}$$

Note that the results (5)-(9) hold regardless of the temperature dependence of B and C, but require that terms in G of order higher than P^6 be negligible.

The temperature derivative of G at constant strain and polarization gives the entropy

$$S = - \partial G/\partial T = - (\tfrac{1}{2} A'P^2 + \tfrac{1}{4} B'P^4 + \tfrac{1}{6} C'P^6 + \ldots) , \qquad (10)$$

where the prime indicates differentiation with respect to temperature. The entropy decrease in going from the non-polar to the polar phase is thus

$$\Delta S = \tfrac{1}{2} A' P_{sc}^2 + \tfrac{1}{4} B' P_{sc}^4 + \tfrac{1}{6} C' P_{sc}^6 + \ldots , \qquad (11)$$

where P_{sc} is the value of P_s at $T = T_c$.

Of course, ΔS is non-zero only for a first-order transition ($B<0$). The latent heat associated with a first-order transition is simply

$$W = T_c \Delta S . \qquad (12)$$

B. Pyroelectricity. The pyroelectric coefficient φ is just the temperature derivative of the spontaneous polarization:

$$\varphi = - \partial P_s/\partial T . \qquad (13)$$

Since P_s satisfies Eq.(2) with $E = 0$, we can differentiate this equation with respect to T and obtain

$$\varphi = \frac{A'P_s + B'P_s^3 + C'P_s^5 + \ldots}{A + 3BP_s^2 + 5C P_s^4 \ldots} = \chi (A'P_s + B'P_s^3 + C'P_s^5 + \ldots), \qquad (14)$$

where the prime again indicates differentiation with respect to temperature.

Various figures of merit have been defined for the operation of pyroelectric detectors[4-6]. Byer and Roundy[5] have shown that the response of a pyroelectric detector in the high-frequency limit is proportional to φ/ϵ, where $\epsilon = 1+4\pi\chi$ is the dielectric constant. So for $\chi \gg 1$ we may define the response figure of merit

$$M_1 = \varphi/\chi \ , \tag{15}$$

and the thermodynamic theory then gives

$$M_1 = A'P_s + B'P_s^3 + C'P_s^5 + \ldots \tag{16}$$

It has also been shown[5,6] that the signal to noise ratio of a pyroelectric detector is proportional to $\varphi/\sqrt{\epsilon}$, implying a noise figure of merit

$$M_2 = M_1 \chi^{\frac{1}{2}} \ . \tag{17}$$

It is clear from Eqs. (14) and (16) that any microscopic model for ferroelectricity, in order to be useful in predicting pyroelectric coefficients and pyroelectric detector performance, must successfully predict the temperature dependence of the Devonshire coefficients. As will be shown below, the lowest-order approximation to Eq.(14), $\varphi = A_o \chi P_s$, does not provide an adequate description for $BaTiO_3$ and is likely to fail for other perovskites as well.

It should be noted here that Eq.(14) is just a special case of the general result

$$\varphi/\chi = (\partial E/\partial T)_P \ . \tag{18}$$

Equation (18) follows from the thermodynamic relation

$$\left(\frac{\partial E}{\partial P}\right)_T \left(\frac{\partial P}{\partial T}\right)_E + \left(\frac{\partial E}{\partial T}\right)_P = 0 \ ,$$

which is valid at constant stress. A general examination of the thermodynamic significance of the pyroelectric coefficient and figure of merit is currently in progress.

III. MICROSCOPIC THEORY

Two distinct types of theory have been developed to describe the ferroelectric phase transition. The more recent and generally fruitful of these is based on the concept of the lattice dynamical instability, or "soft mode", introduced by Cochran[7] and Anderson[8]. This theory assumes the existence of an infrared-active phonon mode whose frequency of vibration is small due to a compensation of the short-range restoring forces by long-range Coulomb interactions. By making reasonable assumptions concerning the temperature dependence of the force constants or by introducing the anharmonicity of the lattice explicitly, one can obtain a soft-mode frequency which vanishes at a characteristic temperature T_o. The crystal then acquires a distortion and polarization of the same symmetry as the soft mode, and the Lydanne-Sachs-Teller relation predicts a Curie-Weiss law for the dielectric constant[7]. The soft-mode theory thus establishes a connection between the macroscopic Devonshire coefficients and microscopic parameters such as inter-atomic force constants and effective charges. Its major drawback in the present context lies in the fact that there do not exist adequate a priori theories for the microscopic parameters involved. Instead, one must infer values of these parameters from the observed values of the macroscopic quantities. Hence in its present state of development the soft mode theory lacks the predictive power needed to relate the pyroelectric behavior of a crystal to its microscopic properties.

In searching for a formalism better suited to the problem at hand we have re-examined older theories based on the mean-field approximation[9]. Such theories describe the ferroelectric phase transition as an order-disorder transformation resulting from the ordering of an array of permanent dipoles, as in the Weiss molecular-field theory of ferromagnetism. This approach would not appear to be applicable to the pervoskites, where the

structure determined for the paraelectric phase (space group O_h^1) has each atom located at an inversion center, thus precluding the existence of permanent dipoles. In addition, the phase transitions predicted by the mean-field theories are of second-order, while many of the perovskites exhibit first-order transitions[2]. The purpose of this section is to show that neither of these objections should be regarded as ruling out the possibility of an adequate description of ferroelectricity in the perovskites based on a mean-field theory. Part A presents experimental evidence for the existence of disorder in the paraelectric phase of the pervoskites, indicating that the atomic sites may be inversion centers only in some average sense and that a consistent interpretation can be given to the dipole moment which appears in the mean-field theories. With the first objection to this approach removed, part B outlines the results of the conventional molecular-field theory, using the Lorentz form for the local field. Part C then introduces a generalized form for the local field which permits the existence of first-order as well as second-order transitions, thus eliminating the second objection mentioned above. Although introduced in an ad hoc way, this local field can be shown to represent a reasonable generalization of the Lorentz field and to correspond in a formal way to a modification of the molecular field introduced by Onsager in order to correct well-known failures of the Lorentz local field in dealing with liquids and solids containing permanent dipole moments.

A. Evidence for Disorder. The first indication of disorder in the pervoskites was obtained from the observation of diffuse scattering of electrons[10] and x-rays[11] in tetragonal $BaTiO_3$. Diffuse scattering was seen in all {100} reciprocal planes except those passing through the origin. Comès et al[12] extended these observation to all four phases of $KNbO_3$ and found that as the temperature was lowered, one set of diffuse scattering

planes disappeared at each phase transition, until the lowest-temperature (rhombohedral) phase exhibited no diffuse scattering. In the ferroelectric phases, scattering was seen only in reciprocal planes perpendicular to those cubic axes which were themselves perpendicular to the spontaneous polarization. This behavior was interpreted by Comès et al[12,13], following a model proposed by Takahasi[14], as arising from correlated displacements of the metal atoms from the centers of the oxygen octahedra. The observed scattering in the cubic phase was accounted for by assuming that each metal atom is displaced along one of the eight equivalent <111> directions in which the displacements along the chain direction are correlated for distances of from 10 to 30 unit cells. Averaged over distances large compared to this correlation length, however, the structure has cubic symmetry. At the cubic-to-tetragonal transition, long-range order appears along one of the cubic axes, which then becomes the tetragonal c-axis (and the direction of spontaneous polarization), while only the short-range order persists in the other <100> directions. The lower-temperature transitions can then be described as the appearance of long-range order along the remaining cubic axes. It is readily shown[13] that this model accounts for the observed form of the diffuse scattering and for its progressive disappearance at each of the transition temperatures.

More recently, similar diffuse scattering patterns have been seen in inelastic neutron scattering experiments[15] on $BaTiO_3$, $KNbO_3$, $KTaO_3$, $KTa_xNb_{1-x}O_3$ (KTN), and $SrTiO_3$. Both neutron scattering and NMR measurements have shown, however, that the displacement correlations are dynamic[16,17], rather than static as originally proposed by Comès et al[12,13]. The dynamic character of the correlations is not an obstacle to the use of an order-disorder model, however. As noted by Yamada et al[18], the neutron scattering

results, which are generally interpreted in terms of an overdamped soft phonon, can be equally well described as a tunneling mode in which the atoms tunnel through a potential barrier between equilibrium positions symmetrically arranged about the center of symmetry. In the latter picture, the unit-cell dipole moment which appears in the molecular field calculations can be interpreted as an instantaneous value (corresponding to one of the equilibrium positions) and the free energy obtained by time averaging has the same form as it would if the dipoles were static.

Further evidence for disorder in the perovskites has been obtained from Ramar scattering measurements[19-21]. No first-order Raman scattering can be produced by a crystal having the cubic perovskite structure, since each atom is located at an inversion center. Yet Fontana and Lambert[19] observed broad scattering peaks in tetragonal $BaTiO_3$ which show no sharp drop in intensity at the cubic-to-tetragonal transition temperature; the integrated intensity of these peaks exhibits a temperature dependence different from that expected for either first- or second-order scattering. Although Barbosa et al[22] have suggested that this peculiar temperature dependence is not intrinsic but rather due to an increase in optical absorption at high temperatures, careful measurements of both absorption and Raman scattering on the same, high-quality sample confirm that the behavior is in fact intrinsic[23].

Fontana and Lambert[19] suggest that these observations could be accounted for if the anomalous features in the Raman spectra are interpreted as disorder-induced first-order scattering, i.e. one-phonon scattering by modes which would not be Raman-active in a perfect crystal but which become so when both the translational and point-group symmetries are broken by the disorder. Since all phonons (not only those at the zone center) can become Raman active in this way, one anticipates a scattering spectrum proportional

(in first approximation) to the one-phonon density of states. We have performed Raman scattering measurements[21] on good quality, single domain orthorhombic $KNbO_3$ crystals (provided by E. Wiesendanger, ETH Zürich), and some of the results are shown in Figs. 1-3. Figure 1 compares the results obtained in two different scattering geometries, $X(YY)\bar{X}$ and $X(ZZ)\bar{X}$. (The notation $\vec{k}_i(\vec{\epsilon}_i\vec{\epsilon}_s)\vec{k}_s$ indicates the directions of the incident and scattered wavevectors $\vec{k}_i$ and $\vec{k}_s$, respectively, and of the polarization vectors of the incident and scattered waves $\vec{\epsilon}_i$ and $\vec{\epsilon}_s$, respectively. The axes are those of the high-temperature cubic phase, with the convention that the spontaneous polarization P_s is along (110).) The two spectra are strikingly different, despite the fact that both involve the same momentum transfer $\vec{k}_s-\vec{k}_i$ and the same symmetry component (A_1) of the Raman tensor[23a]. In the $X(YY)\bar{X}$ geometry, both incident and scattered photons are polarized perpendicular to Z, the direction in which the disordered chains are formed, and the result is a typical first-order spectrum, showing sharp peaks against an essentially negligible background. The $X(ZZ)\bar{X}$ geometry, on the other hand, has both incident and scattered photons polarized parallel to the z-axis, and the resulting spectrum contains, in addition to the peaks seen in the $X(YY)\bar{X}$ spectrum, a broad, relatively featureless background whose intensity is comparable to that of the one-phonon peaks. This background appears to have a maximum near 150 cm^{-1}; as noted by Quittet et al[20], neutron scattering experiments[15] have located a rather flat phonon branch, corresponding to TO modes propagating perpendicular to the z-axis, near this energy which could be responsible for a maximum in the density of states.

Figure 2 illustrates a second interesting aspect of our experimental findings. The geometry $Y(XZ)\bar{Y}$ yields scattering from modes of B_2 symmetry[23a],

which is that of the soft mode responsible for the orthorhombic-to-rhombohedral transition.[15] In the $Y(XZ)\bar{Y}$ spectrum (Fig. 2a), the peak at 39 cm^{-1} has been attributed[20] to a density of states maximum due to the flat TA branch[15] near 50 cm^{-1}. We have found, however, that if the crystal is rotated about its x-axis (see Fig. 2b) this maximum shifts rapidly toward higher energies. A typical spectrum for the rotated crystal, labeled $Y(XZ)\bar{Y} + R$, is shown in Fig. 2a. In this measurement the direction of propagation of the light inside the crystal has been rotated away from the y-axis by less than 12°, but the position of the peak is shifted by nearly 25 cm^{-1}, or more than 50%. This behavior is inconsistent with the assumption that the scattering is due to the one-phonon density of states, and we believe instead that it is produced by a phonon of near-zero wavevector whose frequency-momentum relation is highly anisotropic. It has been shown[15] that the lowest-lying B_2 mode is soft only for wavevectors in the xy-plane, so that as we rotate the momentum transfer $\vec{k}_s - \vec{k}_i$ (and, assuming that crystal momentum is conserved, the wavevector of the emitted phonon) from the y-axis toward the z-axis, we should expect a significant increase in the phonon frequency.

It can be shown, using arguments similar to those of Loudon[23a] for the case of a uniaxial crystal, that if the anisotropy of the short-range force constants is small compared to the electrostatic interactions, the angular dependence of the phonon frequency ω should be given by

$$\omega^2 = \omega_1^2 \sin^2\theta + \omega_2^2 \cos^2\theta \,, \qquad (19)$$

where θ is the angle between the phonon wavevector and the z-axis. We measured ω for external angles of incidence (θ' in Fig. 2b) up to 55°, corresponding to values of θ (assuming a refractive index $n = 2.3$) ranging from 69° to 90°. We also found ω for $\theta = 45^{\circ}$ from spectra taken in the

Y(ZX)Z geometry. The results, indicated by the triangles and square in Fig.3, are in good agreement with the prediction of Eq. (19), shown by the solid curve in Fig. 3. A least-squares fit gives $\omega_1 = 250\ cm^{-1}$ and $\omega_2 = 39\ cm^{-1}$. Unfortunately it is not possible to observe a mode of B_2 symmetry when the momentum transfer is along the z-axis (i.e. $\theta=0$). We have observed, however, that spectra corresponding to A_1 symmetry with momentum transfer along z, e.g. $Z(XX)\bar{Z}$, exhibit a broad peak centered at $250\ cm^{-1}$ and that this peak shifts slowly to lower energy as the crystal is rotated about the x-axis. The angular dependence of this peak in the range $0 \leq \theta \leq 21^{\circ}$ was measured (circles in Fig. 3) and also found to fit Eq. (19). This agreement suggests that we are in fact seeing the same mode in each set of measurements, despite the group theoretical restriction that only B_2 modes should be seen in the $Y(XZ)\bar{Y}$ geometry and only A_1 modes for $Z(XX)\bar{Z}$. Such an explanation is admissible if we note that the group-theoretical selection rules hold only for phonons exactly at the center of the Brillouin zone. The phonons observed in Raman scattering have finite (although small) wavevectors equal to the momentum difference $\vec{k}_s - \vec{k}_i$. At finite wavevector an infra-red active phonon can have mixed symmetry[23a], with atomic displacements equal to a linear combination of displacements transforming according to each of the zone-center symmetries which is infrared active (in this case A_1, B_1, and B_2). The results shown in Fig. 3 suggest that this mixing may be quite strong. The strongest objection to our identification of the $39\ cm^{-1}$ line as the soft mode is that the neutron scattering experiments of Currat et al[15] place the soft mode frequency of about $25\ cm^{-1}$ at room temperature. This discrepancy could be caused by a difference between our sample and theirs in the value of the orthorhombic-to-rhombohedral transition temperature. Unfortunately, the transition temperature was not measured for

either sample, because of the danger of damage to the crystal in passing through a first-order phase transition.

B. Molecular Field Theory. The evidence presented in the previous section strongly suggests the presence of disordered dipoles in all but the lowest-temperature phases of the pervoskites. Lambert and Comès[24] have examined the consequences of assuming that the phase transitions in these materials are of the order-disorder type and concluded that such a description is consistent with experiment. In the following we will re-examine the molecular field theory (MFT) used by Lambert and Comès[24] in order to show that it is in fact not adequate to describe the behavior of the pervoskites and in order to lay the foundations for the generalized molecular field theory to be presented in the following section.

Since the MFT, as applied to ferromagnetism, is treated in most elementary texts on statistical mechanics[25], we will simply summarize the results obtained in the case of ferroelectricity.

The instantaneous energy of orientation of an electric dipole moment $\vec{\mu}$ is given by

$$H = - \vec{\mu} \cdot \vec{E}_\ell \qquad (20)$$

where $\vec{E}_\ell$ is the local field acting on the dipole. The usual MFT is obtained by assuming that the local field has the Lorentz form

$$\vec{E}_\ell = \vec{E} + \frac{4\pi}{3} \vec{P} \quad , \qquad (21)$$

where $\vec{E}$ is the applied (macroscopic) electric field, and $\vec{P}$ is the macroscopic polarization. If we consider a cubic (or isotropic) medium (so that $\vec{P}$ is parallel to $\vec{E}$) and assume that the dipole moment can rotate freely, the usual statistical arguments for an array of N independent dipoles give

$$P(T) = N\mu \, L(x) \, , \qquad (22)$$

where

$$L(x) = \coth x - 1/x \text{ and } x = \mu E_\ell / kT \tag{23}$$

(k is Boltzman's constant).

For small values of x, L(x) can be expanded in a power series

$$L(x) = \frac{1}{3} x - \frac{1}{45} x^3 + \frac{2}{945} x^5 + \dots , \tag{24}$$

and this series can be inverted to give

$$x = 3y + \frac{9}{5} y^3 + \frac{297}{175} y^5 + \dots , \tag{25}$$

where $y = L(x) = P/N\mu$. Equation (25) which relates E_ℓ and P, can be solved for E to give

$$E = A_o(T-T_c) P + BP^3 + CP^5 + \dots , \tag{26}$$

where

$$\begin{aligned} A_o &= 3k/N\mu^2 \\ B &= 3A_o T/N^2\mu^2 \\ C &= 99A_o T/175\ N^4\mu^4, \text{ etc.} \end{aligned} \tag{27}$$

and

$$T_o = 4\pi/3A_o . \tag{28}$$

Since the electric field (26) has the same form as Eq. (2), we obtain a free energy of the Devonshire form

$$G = \tfrac{1}{2} A_o(T-T_o) P^2 + \tfrac{1}{4} BP^4 + \tfrac{1}{6} CP^6 + \dots . \tag{29}$$

An important property of the free energy (29) is that the coefficient of P^4, $B = 3A_o T/N^2\mu^2$, is positive for all finite temperatures. Hence the MFT predicts a second-order phase transition. This conclusion is not altered

if one replaces the assumption that the dipole moment can rotate freely by the requirement that it be either parallel or antiparallel to the applied field[24] or that it have one of a set of possible orientations consistent with the cubic symmetry[6]. The addition to Eq. (22) of an induced polarization[26] αE_ℓ, proportional to the molecular polarizability α, also has no effect on the order of the phase transition. The observation of first-order transitions in the pervoskites casts serious doubt on the validity of a MFT based on Eq. (21). Since the theory predicts a second-order transition which has no latent heat, to attempt, as do Lambert and Comès[24], to identify the saturation polarization $P_{sat} = N\mu$ with the spontaneous polarization at T_c and to calculate the latent heat from Eqs. (11) and (12) is to distort the conclusions of the MFT.

Before discussing our proposed generalization of the MFT, we should note two other consequences of the MFT which are frequently considered objectionable[27]. First, Eq. (28) implies that $A_o T_o = 4\pi/3$, while in every case in which A_o and T_o have been measured in a pervoskite, one finds $A_o T_o \ll 4\pi/3$. The theory thus requires a Lorentz factor in Eq. (21) which is substantially smaller than $4\pi/3$. However, the Lorentz factor varies rapidly with position in the perovskite unit cell[28] so that the finite extent of the dipoles (or the finite displacement of the equilibrium positions of the ions from the cubic lattice sites) may produce a substantial reduction of the Lorentz factor. A second objection arises from the fact that if each unit cell contains an independent dipole, the entropy change produced by the ordering will be of the order of k per unit cell, while experiments indicate a value which is smaller by at least an order of magnitude[27]. This difficulty can be met if the x-ray results are interpreted to mean that the independent dipoles are actually chains of length 10-30 unit cells. The entropy change is then reduced to approximately the observed value[24], although the conventional MFT continues to

predict a second-order transition.

C. Generalized Molecular Field Theory. We will now describe a generalized molecular field theory (GMFT), which, by permitting a first-order phase transition, overcomes the main objection raised to the conventional MFT. The GMFT is obtained by simply replacing the Lorentz local field (21) with a local field of the form

$$E_\ell = E + \lambda P + \lambda' P^3 + \lambda'' P^5 + \ldots \quad . \tag{29}$$

We have used the cubic symmetry of the crystal and the assumption that the polarization occurs along a cubic axis in order to suppress the tensor nature of $\lambda, \lambda', \lambda'', \ldots$ and permit them to be written as simple coefficients. With this modification of the local field, Eq. (25) now gives

$$E = A_o(T-T_o)P + B_o(T-T_1)P^3 + C_o(T-T_2)P^5 + \ldots \quad , \tag{30}$$

where

$$\begin{aligned} A_o &= 3k/N\mu^2 \quad , & T_o &= \lambda/A_o \\ B_o &= 3A_o/5N^2\mu^2 \quad , & T_1 &= \lambda'/B_o \\ C_o &= 99\, A_o/175\, N^4\mu^4 \quad , & T_2 &= \lambda''/C_o \end{aligned} \tag{31}$$

and so forth. This leads to the free energy

$$G = \tfrac{1}{2} A_o(T-T_o)P^2 + \tfrac{1}{4} B_o(T-T_1)P^4 + \tfrac{1}{6} C_o\,(T-T_2)P^6 + \ldots \quad . \tag{32}$$

One sees immediately that for $T_1 > T_o$ the coefficient of P^4 ,

$$B = B_o\,(T-T_1) \quad , \tag{33}$$

will be negative in the vicinity of T_o, and a first-order transition is possible. The temperature dependence of B has been measured only in

$BaTiO_3$. Drougard et al[29] studied the polarization dependence of $1/\chi$ in the paraelectric phase and found that B has the predicted form (33) with $B_o = 1.8 \times 10^{-14}$ cgs and T_1 448 K. Also, Huibregtse and Young[30] determined B from measurements of the susceptibility and spontaneous polarization in the ferroelectric phase (just above the tetragonal-orthorhombic transition) and found a value in good agreement with Eq.(33) using the parameters given by Drougard et al[29]. More recently, the work of Matsuda and Abe[31] has failed to confirm Eq. (33), but these measurements yield B only indirectly, via a calculation which makes the dubious assumption that C is temperature-independent.

Before entering into a detailed examination of the consequences of the free energy (32) predicted by the GMFT, we will discuss briefly the question of the local field in order to justify the form proposed in Eq. (29). It has long been known[32] that the Lorentz local field (21) is not suitable for the description of liquids composed of polar molecules (i.e. molecules having permanent electric dipole moments). The reason is that if the observed densities and molecular dipole moments are substituted in Eqs. (27) and (28) the MFT predicts that one should observe ferroelectric ordering in many common liquids at room temperature. (Water, for example[32], would order at T_o = 1140 K.)

Among the numerous attempts to avoid this difficulty in the MFT, one finds a particularly interesting and elegant approach due to Onsager[33]. Consider a medium of dielectric constant ϵ in an applied electrid field $\vec{E}$. The field inside a spherical cavity of radius a containing a single dipole of moment $\vec{\mu}$ can be calculated as follows[34]. For $\vec{\mu} = 0$ the applied field produces a field in the cavity, $\vec{G} = \frac{3\epsilon}{2\epsilon+1} \vec{E}$. The presence of the dipole

gives rise to an additional field $\vec{R} = \frac{\epsilon-1}{2\epsilon+1} \frac{2}{a^3} \vec{\mu}$. This "reaction field" is the difference between the field which the dipole would produce in vacuum and that actually produced in the medium. The field in the cavity is then the field of the dipole itself plus the sum $\vec{G}+\vec{R}$. If $\vec{\mu}$ were an induced dipole it would be related to the macroscopic polarization by $\vec{P} = \vec{\mu}/V$, where $V = \frac{4}{3} \pi a^3$, and one would obtain the Lorentz result, $\vec{G}+\vec{R} = \vec{E} + 4\pi/3 \vec{P}$. For a permanent dipole, however, Onsager[33] pointed out that since $\vec{R}$ is always parallel to $\vec{\mu}$, the only field tending to orient $\vec{\mu}$ parallel to $\vec{P}$ is the cavity field $\vec{G}$. Thus the local field appearing in the orientation energy (20) should be $\vec{E}_\ell = \vec{G}$ or

$$\vec{E}_\ell = \vec{E} + \frac{4\pi}{2\epsilon+1} \vec{P} , \tag{34}$$

where we have used $\vec{P} = \chi\vec{E} = \frac{\epsilon-1}{4\pi} \vec{E}$. If $\epsilon \gg 1$, we have $4\pi/(2\epsilon+1) \simeq 1/2\chi$, and the Devonshire result for the dielectric stiffness (3) gives

$$E_\ell = E + \tfrac{1}{2} AP + \frac{3}{2} BP^3 + \frac{5}{2} CP^5 \ldots . \tag{35}$$

Thus in a ferroelectric the Onsager local field is not linear in the polarization but contains terms of all orders in P. While Eq. (35) can be regarded as a special case of (29), several points should be kept in mind. In our development we have assumed implicitly that the coefficients $\lambda,\lambda',\lambda'',\ldots$ are temperature-independent. This is not the case for the Onsager field (35), and the consequences are interesting. Although Onsager believed that Eq.(35) does not lead to a phase transition since the dielectric constant cannot diverge[33], it was later shown[35] that there is in fact a first-order transition but without a Curie-Weiss behavior of the dielectric constant. Pirenne[35] has compared the Lorentz and Onsager forms of the local field in terms of the degree of correlation among the dipoles which they imply. The Lorentz form assumes no correlation: the

dipoles of the medium do not respond to the orientation of the test dipole, so that the reaction field is always equal to $\frac{8\pi}{3}\ \frac{\epsilon-1}{2\epsilon+1}\vec{P}$. On the other hand, the Onsager formula assumes "complete" correlation: the medium is always polarized in a way consistent with the instantaneous orientation of the test dipole, so that $\vec{R}$ is always parallel to $\vec{\mu}$. Since processes involving the rotation of dipoles or the tunneling of ions are generally much slower than electronic processes, one might expect the real situation to lie somewhere between these two extremes. Finally, Fröhlich[33] has pointed out that in deriving either form of the local field one neglects short-range forces and considers only long-range, dipole-dipole interactions. Yet lattice dynamical calculations[36] indicate that short-range forces play a significant role in the correlations which lead to the formation of chains. They are also likely to affect the interaction between chains, causing a departure from the simple dipole-dipole interaction assumed in deriving the Onsager result (34). In summary, the proposed form (29) for E_i resembles the Onsager result in that its nonlinear dependence on P permits the existence of a first-order transition, while the introduction of the $\lambda,\lambda',\lambda''$, ... as adjustable parameters permits the theory to take into account the short-range forces in an empirical way. Calculations are now under way in an attempt to relate the expansion coefficients $\lambda,\lambda',\lambda''$, ... to the microscopic quantities which determine the dynamic behavior of the lattice.

In order to compare the predictions of the free energy G (32) with experiment, we note first that the coefficients A_o, B_o, C_o, ... given by Eq. (31) depend on just two parameters, N and μ. If we ignore terms in G of order higher than P^6, we have only three additional parameters, the temperatures T_o, T_1, and T_2. For $BaTiO_3$, four of these quantities have been determined directly from experiment:[29,37]

$$A_o = 7.6 \times 10^{-5} \text{ cgs} \quad , T_o = 383 \text{ K}$$
$$B_o = 1.8 \times 10^{-14} \text{ cgs} \quad , T_1 = 448 \text{ K} \tag{36}$$

We obtain from these the number of independent dipoles, $N = A_o^2/5kB_o = 4.6 \times 10^{20}$ cm^{-3} and the saturation polarization $P_{sat} = N\mu = (3A_o/5B_o)^{\frac{1}{2}} = 17$ μC/cm^2. The observed density of $BaTiO_3$ gives $N_o = 1.5 \times 10^{22}$ unit cells/cm^3, so that the calculated value of N corresponds to a chain length $L = N_o/N = 33$ unit cells, which is quite consistent with the observed width of the diffuse x-ray scattering streaks[12,13]. Experimental estimates of the saturation polarization lie in the range 16-26 μC/cm^2, depending on the quality of the sample[29]. Our calculated value of P_{sat} is somewhat low, especially since the data (36) are for a sample with a relatively large spontaneous polarization, but the agreement with experiment is still satisfactory. In principle, one more piece of experimental data would be required for each of the additional characteristic temperatures $T_2, T_3, \ldots$ we wish to determine. We can proceed in an approximate way, however, if we note that the observed values of P_s near the Curie point are quite close to our calculated P_{sat} and that, as noted elsewhere[38], the approach of P_s to its saturation value as the temperature is lowered is much more rapid than is predicted by Eq.(5) with constant values of B and C. These observations suggest that if we ignore terms in G of order higher than P^6, we should approximate P_s at $T = T_c$ by P_{sat}, so that Eq.(6) gives

$$\sigma = -44/35 \quad , \text{ at } T = T_c \quad , \tag{37}$$

where $\sigma = (T-T_1)/(T-T_2)$. Evaluating Eq.(5) at the Curie point gives

$$\tau/\sigma = 21/176 \quad , \text{ at } T = T_c \quad , \tag{38}$$

where $\tau = (T-T_o)/(T-T_1)$. Equation (38) yields

$$T_c = \frac{176\, T_o - 21\, \sigma_c T_1}{176 - 21\, \sigma_c} \quad , \tag{39}$$

where the subscript c indicates $T = T_c$. Substituting the approximation (37) and the experimental data (36) in Eq. (39) gives

$$T_c = (20T_o + 3T_1)/23 = 391.5 \text{ K} \, , \tag{40}$$

which is in excellent agreement with the observed Curie temperature[29,37], $T_c = 392$ K. We must point out, however, that the approximation (37) also leads to

$$T_2 = [(\sigma_c - 1)\, T_c + T_1]/\sigma_c = 346.5 \text{ K} \, . \tag{41}$$

When the free energy (with $B < 0$) is truncated at the P^6 term, it no longer has a stable minimum at $P = P_s$ if $C = C_o(T - T_2)$ vanishes. (See Section II). Hence the temperature T_2 is a lower bound for the validity of the assumption that the higher-order terms are negligible, and we find that results depending on this assumption, such as Eqs. (5) and (14), can be correct in at most the limited range $T_c - T \leq 45$ K. In fact, even close to the Curie point there is evidence for the importance of higher-order terms: Eq. (9), relating the susceptibilities of the paraelectric and ferroelectric phases $\chi_p = 4\chi_f$, is not well satisfied[39]. If, despite these warnings, we continue to neglect the higher-order terms, we obtain from Eqs. (11) and (16) the entropy change at T_c

$$\Delta S = \tfrac{1}{2} A_o P_{sc}^2 + \tfrac{1}{4} B_o P_{sc}^4 + \tfrac{1}{6} C_o P_{sc}^6 \, , \tag{42}$$

and the response figure of merit,

$$M_1 = A_c P_s + B_o P_s^3 + C_o P_s^5 \, . \tag{43}$$

The predictions of Eqs. (42) and (43), with $P_s = P_{sc} = P_{sat}$, are compared with experiment[2,27,40] in Table I, which summarizes the experimental tests of the GMFT. The overall agreement for $BaTiO_3$ is quite good, despite possible errors arising from the truncation of the power series for G. We are currently attempting to estimate the magnitudes of such errors and to find methods of calculation which avoid them.

As noted in Section I, the GMFT leads to contributions to φ and M_1 from the temperature dependence of B and C, and these are not negligible. For example, if B and C are assumed temperature-independent, one obtains $M_1 = A_o P_s = 3.9$, which is less than half the result given by Eq. (43) and substantially less than the experimental figure of merit (see Table I). It is also worth pointing out the important role of the local field in determining M_1. From Eq.(43), together with Eq.(2) and the observation that E=0 for $P=P_s$, we obtain

$$M_1 = \frac{1}{T} (\lambda P_s + \lambda' P_s^3 + \lambda'' P_s^5 + \dots) , \qquad (44)$$

where we can recognize that the term in parentheses is equal to E_t for E=0. The first term of (44), $M_1 = A_o T_o P_s/T$, was obtained from the conventional MFT by van der Ziel[6], who concluded that the factor T_o/T implied that increased Curie temperatures would result in improved room-temperature detectivity. In fact, the correct temperature dependence of M_1 is given by Eq. (43): M_1 depends on temperature only through P_s. The 1/T dependence given by (44), while correct, is misleading since it reflects the fact that the orientational contribution to χ vanishes as the polarization saturates. Detector performance is then limited by electronic contributions to χ which are not included in the model.

IV. PRESENT STATUS AND FUTURE PLANS

A. Experimental - In addition to our continuing investigation of Raman scattering in $KNbO_3$, measurements are now in progress on $BaTiO_3$ and $LiTaO_3$. In $KNbO_3$ we have obtained spectra exhibiting line shapes characteristic of resonant interference, similar to the results of Rousseau and Porto[41] for $BaTiO_3$. We are currently in the process of fitting and interpreting these spectra with the aid of the theory developed by Fano[42] for Auger processes. An interesting preliminary observation is that the interference seems to involve a sharp line of (predominantly) A_1 symmetry at about 195 cm^{-1} and the same broad, strongly orientation dependent peak discussed in Section III A. If our interpretation of this latter feature is correct, we are seeing interference between scattering processes involving two different one-phonon final states[43], not a one-phonon state and a two-phonon state as proposed by Rousseau and Porto[41].

We have also begun a second series of experiments designed to explore the nature of the disorder in the perovskites. We plan to measure optical second harmonic generation (SHG)[44] as a function of temperature near the cubic-to-tetragonal transition. Since the cubic perovskite structure has inversion symmetry, a perfectly ordered crystal having this structure would produce no SHG[44]. Thus observation of SHG in the high-temperature phase would add to the evidence favoring the existence of disorder, and its spatial distribution would contain information concerning any correlations of the atomic displacements. SHG measurements below the transition temperature will be of value also, since only a limited amount of data on the temperature dependence of the SHG coefficients is available[45]. Simple theoretical models[46] suggest that these coefficients should be directly proportional to the antisymmetric part of crystalline potentional and hence to P_s. This behavior has been found in $BaTiO_3$ and $LiTaO_3$ but

has not been verified in general[45]. The linear electro-optic coefficient, another nonlinear optical coefficient similar to the SHG coefficient but describing the mixing of photons one of which has zero frequency[47], can also be shown to be proportional to P_s in the models employed in Ref. 46. If we keep only the first term in the expansion (14) for the pyroelectric coefficient φ, we obtain the proportionality between the pyroelectric and linear electro-optic coefficients proposed by Soref[48]. Equation (14) shows that this proportionality should fail when P_s approaches its saturation value, and higher-order terms in φ become important. We intend to pursue, both theoretically and experimentally, these relations between the pyroelectric and nonlinear optical coefficients.

B. Theoretical. The GMFT proposed in Section III lends itself to extension and improvement in two distinct areas defined by the structure of the theory. As one can see from Eq. (31), the coefficients $A_o, B_o, C_o, \ldots$ depend only on the parameters N and μ and our choice of the function $L(x) = \coth x - 1/x$. On the other hand, the temperatures $T_o, T_1, T_2, \ldots$ depend on the local field as well as on the coefficients $A_o, B_o, C_o, \ldots$. It therefore makes sense to consider separately the problem of determining the temperatures and that of determining the coefficients since, while not independent, the two problems are coupled in a particularly simple way. Our ultimate goal is to relate all these parameters to microscopic quantities which can be obtained from either experimental or theoretical descriptions of the lattice dynamics of the pervoskites.

Calculation of the coefficients in Eq.(31) can itself be divided into two subproblems. The parameters N and μ can be obtained from lattice dynamics calculations since the former is related to the correlation length characteristic of the chains[36], and the latter can be calculated from the

effective ionic charges used in the calculation and the atomic displacements observed below the phase transition. Since lattice dynamics calculations generally require the input of a substantial number of experimentally determined parameters, we do not regard this approach as inherently superior (or more fundamental) than our procedure in Section III of taking the coefficients A_o and B_o directly from experiment. The higher-order coefficients C_o, etc. then depend on the choice of $L(x)$, which introduces our second subproblem. The present work has used $L(x) = \coth x - 1/x$, which corresponds to the classical or "infinite-spin" limit in which the dipole is free to assume any arbitrary orientation with respect to the applied field. The assumption of Comès et al[12,13] that in the cubic phase the unit cell dipole orientations are equally divided among the $\langle 111 \rangle$ directions leads to a correspondence with the spin $\frac{1}{2}$ case, in which $L(x) = \tanh x$. We have found, however, that this assumption for $L(x)$ leads to poorer agreement with experiment than the classical one and that the gross features of the diffuse x-ray scattering can be explained using other assumptions for the possible orientations of the unit cell dipoles. We are now exploring systematically the consequences of assuming possible dipole orientations corresponding to higher spin values. It is important to note, however, that van der Ziel[6], using a conventional MFT and the assumption that the dipoles may be parallel or anti-parallel to each of the cubic axes, has obtained a partition function, and hence an expression for $L(x)$, which does not correspond to that obtained for any value of the spin. Thus the catalogue of spins $J = \frac{1}{2}, 1, \ldots, \infty$ does not exhaust the list of acceptable partition functions, and we are now seeking both a method of parametrizing the complete set of such partition functions and a physical argument, perhaps based on the details of the diffuse x-ray scattering,

which will determine unambiguously the correct choice.

Calculation of the temperatures in Eq.(31) involves the local field E_ℓ and here we are exploring an approach which, while still speculative, seems at present to be very promising. The local field (29) is given to us as a power series in P, where the coefficients must be determined from experiment. If this expansion is regarded as merely an approximation, it is reasonable to examine other functional forms for E_ℓ which yield Eq. (29) as an expansion for small values of P. One set of possibilities is provided by the theory of Padé approximants[49]. Instead of Eq. (29) we can write

$$E_\ell = E + [m,n] \ , \tag{44}$$

where $[m,n] = p_m/q_n$, the (m,n) Padé approximant for the power series $\lambda P + \lambda' P^3 + \lambda'' P^5 + \ldots$, is the ratio of polynomials p_m and q_n which are of order m and n in P, respectively. The approximant [m,n] agrees with the series up to the term of order P^{m+n}. The lowest-order non-trivial approximant is [2,2] which gives

$$E_\ell = E + \frac{\lambda P}{1-(\lambda'/\lambda)P^2} \ . \tag{45}$$

This agrees with Eq. (29) up to the term in P^4 (which happens to vanish) and predicts

$$\lambda'' = \lambda'^2/\lambda \ . \tag{46}$$

Using the experimental data (35) and Eq.(31) we obtain $\lambda'' = (B_o T_1)^2/A_o T_o = 2.23 \times 10^{-22}$. This is to be compared with the result of the GMFT with $L(x) = \coth x - 1/x$, which gives $C_o = 11\, B_o^2/7A_o$, $T_2 = 346.5$ K (Eq.(41)), and $\lambda'' = C_o T_2 = 2.32 \times 10^{-22}$. This agreement of better than 5% is strong evidence that the coefficients of P in the expansion of E_ℓ(29) are not

independent but are related as implied by Eq.(45). Equation (45) poses an important question, however, which is to justify on physical grounds the presence of a pole in E_ℓ and to determine its location. The smooth dependence of P_s on temperature would rule out the possibility of a pole for $P < N\mu = P_{sat}$. If we make the assumption, as yet unjustified, that the pole occurs at $P = P_{sat}$, we obtain

$$P_{sat} = (\lambda/\lambda')^{\frac{1}{2}} \tag{47}$$

The experimental data (36) then give $P_{sat} = 20\ \mu G/cm^2$ in reasonable agreement with the prediction of the GMFT and with experiment (Table I). The success of Eqs. (46) and (47) suggests that Eq. (45) contains an important insight into the behavior of the local field, but this result remains to be established on a sound physical basis.

V. SUMMARY

The work described in this report was undertaken with the goal of improving our basic knowledge of the phenomenon of pyroelectricity in a way which would lead to practical guidelines for the selection of infrared detector materials and to an understanding of the factors limiting the performance of pyroelectric detectors. The pervoskite family, an extensively studied group of isomorphous materials, was chosen as the object of this investigation both for its simple crystal structure and for the range of physical properties exhibited by its members.

We have developed a theoretical treatment of pyroelectricity in the pervoskites which is based on the connection between pyroelectricity and ferroelectricity in these materials (Section II). With the aid of this theory it was shown that the figure of merit commonly used to characterize pyroelectric detectors is not merely an empirical quantity but one of fundamental thermodynamic significance. This opens the way to an analysis which may lead to a priori limitations on detector efficiency. The theory also permits the figure of merit to be calculated using measurements of the static dielectric constant above the Curie temperature instead of the more difficult direct measurements of the pyroelectric coefficient and dielectric constant below the Curie point.

We have also devised a simple microscopic model (Section III), a generalization of the molecular field theory so familiar in ferromagnetism, which accurately describes the ferroelectric phase transition using only a small number of experimentally accessible parameters. This model not only predicts the ferroelectric and pyroelectric behavior of interest in the present work but is broadly applicable to structural and magnetic

phase transitions of all types. It is simple to use and likely to be of value in many problems involving phase transitions. The model has basic features which are quite novel, and it represents an interesting contribution to the general theory of phase transitions.

Finally, we have performed Raman scattering measurements on $KNbO_3$ which reveal unexpected, anomalous features that cannot be explained in terms of the conventional view of the structural phase transition but which are fully consistent with our generalized molecular field theory.

References

1. A.F. Devonshire, Advan. Phys. 3, 85 (1954).
2. See, for example, E. Fatuzzo and W.J. Merz, in Selected Topics in Solid State Physics, ed. by E.P. Wolforth (J. Wiley and Sons, New York, 1967), vol. 7, Chap. 3.
3. C. Kittel, Phys. Rev. 82, 729 (1951).
4. E.H. Putley, in Semiconductors and Semimetals, ed. by R.K. Willardson and A.C. Beer (Academic Press, New York, 1970) vol. 5, p. 259.
5. R.L. Byer and C.B. Roundy, Ferroelectrics 3, 333 (1972).
6. A. van der Ziel, Final Report on ARPA Contract DAAK 02-72-C-0398, Univ. of Minnesota, April 1974.
7. W. Cochran, Advan. Phys. 9, 387 (1960).
8. P.W. Anderson, in Fizika Dielekrikov, ed. by G.I. Skaravi (ed. Acad. Nuak SSSR, Moscow, 1960) p. 290.
9. See W. Känzig, Solid St. Phys. 4, 1 (1957).
10. G. Honjo, S. Kodera, and N. Kitamura, J. Phys. Soc. Jpn. 19, 351 (1964).
11. J. Horada and G. Honjo, J. Phys. Soc. Jpn 22, 45 (1967).
12. R. Comès, M. Lambert, and A. Guinier, Compt. Rend. 266, 959 (1968).
13. R. Comès, M. Lambert, and A. Guinier, Solid St. Comm. 6, 715 (1968).
14. H. Takahasi, J. Phys. Soc. Jpn. 16, 1685 (1961).
15. See R. Currat, R. Comès, B. Dorner, and E. Wiessendanger, J. Phys. C 7, 2521 (1974), and refs. cited therein.
16. R. Comès and G. Shirane, Phys. Rev. B 5, 1886 (1972).
17. G. Zaccai and A.W. Hewat, J. Phys. C. 7, 15 (1974).
18. Y. Yamada, G. Shirane, and A. Linz, Phys. Rev. 177, 848 (1969).
19. M.P. Fontana and M. Lambert, Solid St. Comm. 10, 1 (1972).
20. A.M. Quittet, M. Lambert, M. Fontana, and E. Wiesendanger, Compt. Rend. 277, 523 (1973).

21. A.M. Quittet, M.I. Bell, and P.M. Raccah, unpublished.

22. G.A. Barbosa, A. Chaves, and S.P.S. Porto, Solid St. Comm. 11, 1053 (1972).

23. A.M. Quittet and M. Lambert, Solid St. Comm. 12, 1053 (1973).

23a. R. Loudon, Adv. Phys. 13, 423 (1964).

24. M. Lambert and R. Comès, Solid St. Comm. 7, 305 (1969).

25. See, for example, F. Reif, Fundamentals of Statistical and Thermal Physics (McGraw-Hill, New York, 1965) chap. 10.

26. W.P. Mason and B.T. Mathias, Phys. Rev. 74, 1622 (1948).

27. See, for example, F. Jona and G. Shirane, in Int. Series of Monographs on Solid St. Phys., ed. by R. Smoluchowski and N. Kurti (Macmillan, New York, 1962) vol. 1, chap. IV.

28. J.M. Luttinger and L. Tisza, Phys. Rev. 70, 954 (1946); 72, 257 (1947).

29. M.E. Drougard, R. Landauer, and D.R. Young, Phys. Rev. 98, 1010 (1955).

30. E.J. Huibregtse and D.R. Young, Phys. Rev. 103, 1705 (1956).

31. T. Matsuda and R. Abe, J. Phys. Soc. Jpn. 34, 418 (1973).

32. See for example, C.P. Smyth, Dielectric Behavior and Structure (McGraw-Hill , New York, 1955) Chap. I.

33. L. Onsager, J. Am. Chem. Soc. 58, 1486 (1936).

34. A detailed discussion of Onsager's calculation can be found in H. Fröhlich, Theory of Dielectrics (Oxford, 1958).

35. J. Pirenne, Helv. Phys. Acta 22, 479 (1949).

36. A. Müller, Solid St. Comm. 7, 589 (1969).

37. M.E. Drougard and E.J. Huibregtse, IBM J. Res. Devel. 1, 318 (1957). See also ref. 27.

38. S. Triebwasser, Phys. Rev. 101, 993 (1956).

39. W.J. Merz, Phys. Rev. 76, 1221 (1949); M.E. Drougard and D.R. Young, Phys. Rev. 95, 1152 (1954).

40. A.G. Chynoweth, J. Appl. Phys. 27, 78 (1956).

41. D.L. Rousseau and S.P.S. Porto, Phys. Rev. Letters 20, 1354 (1968).

42. U. Fano, Phys. Rev. 124, 1866 (1961).

43. J.F. Scott, Revs. Mod. Phys. 46, 83 (1974).

44. See, for example, N. Bloembergen, Nonlinear Optics (W.A. Benjamin, New York, 1965).

45. A.M. Glass, Phys. Rev. 172, 564 (1968) and private communication from R.C. Miller cited therein.

46. See, for example, M.I. Bell, Phys. Rev. B 6, 516 (1972).

47. M.I. Bell, in Proc. 11th Int. Conf. Phys. Semiconductors (Polish Scientific Publishers, Warsaw, 1972), p. 845.

48. R.A. Soref, IEEE J. Quant. Elec. QE-5, 126 (1969).

49. See, for example, M.A. Snyder, Chebyshev Methods in Numerical Approximation (Prentice-Hall, Englewood Cliffs, N.J., 1966) chap. 4.

Table I. Comparison of predictions of the GMFT with experimental results from Refs. 2, 27 and 40.

	Theory	Experiment
P_{sat} ($\mu C/cm^2$)	17	16-26
T_c (K)	391.5	392
ΔS (k/unit cell)	0.03	0.011-0.06
W (cal./mole)	24	9-47
M_1 (cgs)	8.5 ($P_s=P_{sat}$)	10 (373 K)

Figure Captions

Fig. 1. Comparison of $KNbO_3$ Raman spectra for the scattering geometries $X(YY)\bar{X}$ and $X(ZZ)\bar{X}$, showing disorder-induced one-phonon scattering for incident and scattered photons polarized along the z-axis (direction of chain formation).

Fig. 2. (a) Raman spectra of $KNbO_3$ for the scattering geometry $Y(XZ)\bar{Y}$ and for the same geometry but with the crystal rotated by $\theta'=27^{\circ}$ about the x-axis. The latter spectrum is labeled $Y(XZ)\bar{Y}$ + R.

(b) Scattering geometries for the spectra in (a), showing the internal and external propagation angles θ and θ', respectively.

Fig. 3. Angular dependences of the Raman scattering peaks observed at 39 cm^{-1} in the $Y(XZ)\bar{Y}$ geometry and at 250 cm^{-1} in the $Z(XX)\bar{Z}$ geometry. The solid line is the prediction of Eq. (19).

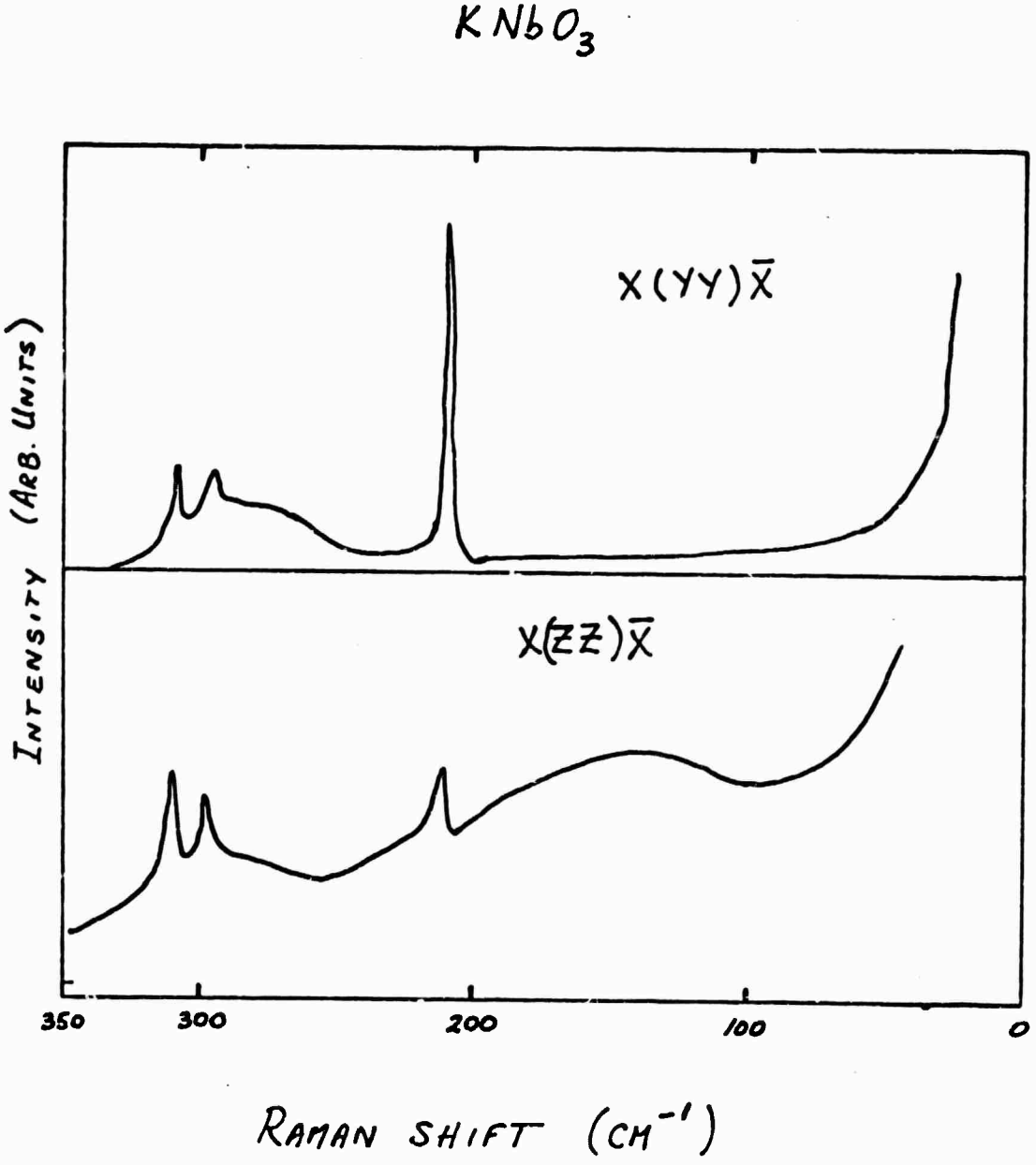
$KNbO_3$
X(YY)$\bar{X}$
X(ZZ)$\bar{X}$
INTENSITY (ARB. UNITS)
350
300
200
100
0
RAMAN SHIFT (CM^{-1})

Fig. 1

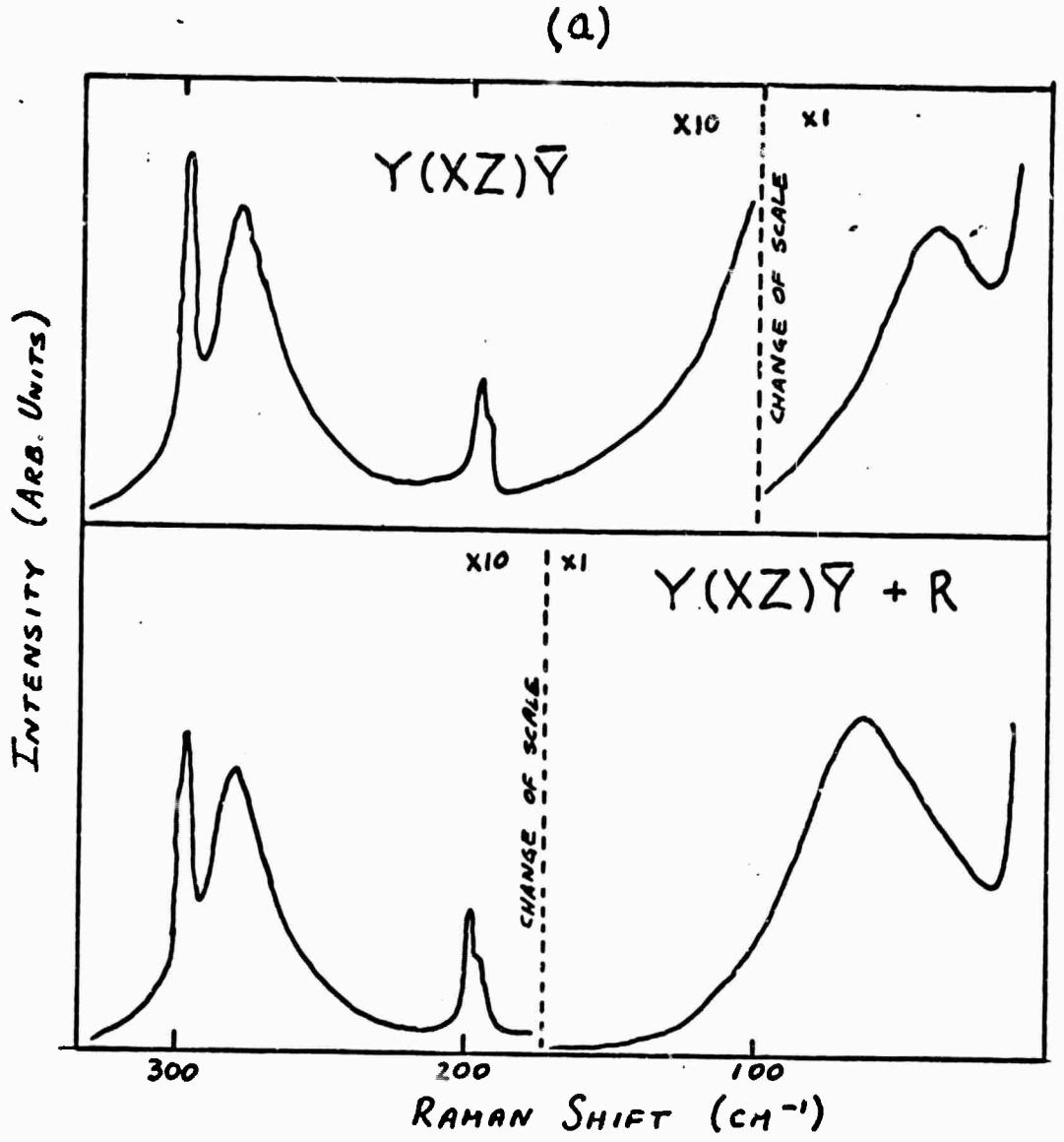
(a)
X10
X1
Y(XZ)Ȳ
CHANGE OF SCALE
X10
X1
Y(XZ)Ȳ + R
CHANGE OF SCALE
INTENSITY (ARB. UNITS)
300
200
100
RAMAN SHIFT (CM⁻¹)

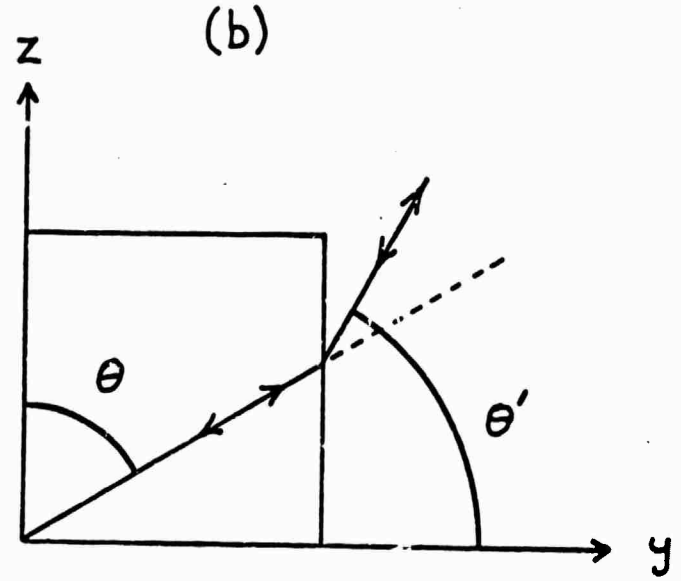
(b)
z
θ
θ'
y

Fig. 2

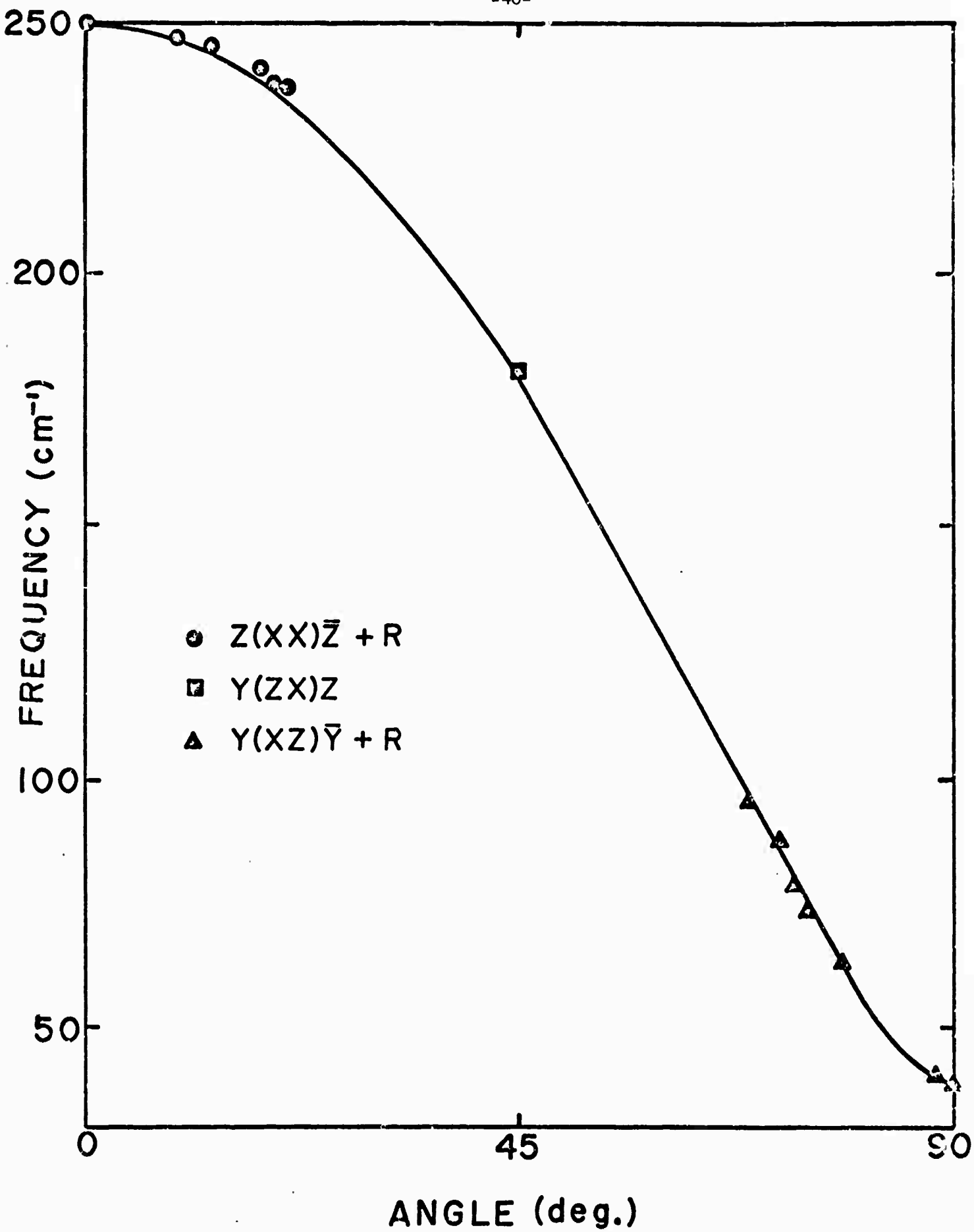
250
200
100
50
FREQUENCY (cm⁻¹)
Z(XX)Z̄ + R
Y(ZX)Z
Y(XZ)Ȳ + R
0
45
90
ANGLE (deg.)

Fig. 3